Preparation and study of YSTZ-Al$_2$O$_3$ nanocomposites

R. N. VISWANATH, S. RAMASAMY
Department of Nuclear Physics, School of Physical Sciences, University of Madras, Guindy Campus, Chennai 600 025, India

Yttria stabilized zirconia-alumina (YSTZ-Al$_2$O$_3$) nanocomposite system with various Al$_2$O$_3$ concentrations has been synthesized by sol-gel route. The experimental techniques XRD, DTA, TGA, FT-Raman, FT-IR, SEM, Vicker's hardness measurements, density measurements and Impedance spectroscopy were used to characterize the synthesized specimens. DTA result shows two exothermic reactions: one around 760 °C and another around 960 °C. XRD results confirm that the specimen starts to crystallize on heating above 750 °C. Well resolved XRD reflections corresponding to tetragonal (t) ZrO$_2$ were obtained after the specimens were heated at 1000 °C. FT-Raman results confirmed that the crystallites developed above 750 °C was t-ZrO$_2$. It was observed from the XRD and DTA results that the bulk and grain boundary region crystallize independently in two different temperatures with a difference in temperature of about 200 °C. The crystallization temperatures increase with Al$_2$O$_3$ contents. At 1300 °C, the pure YSTZ and 5 and 10 wt % Al$_2$O$_3$ added YSTZ specimens underwent structural transformation from tetragonal to monoclinic ZrO$_2$. But, the tetragonal symmetry remains stable at 1300 °C with an addition of 15 wt % Al$_2$O$_3$. The system which retain its tetragonal symmetry at its processing temperature ($\approx$1300 °C) gives high hardness and maximum density values. Almost 100% theoretical density value was obtained at 1300 °C with an addition of 15 wt % of Al$_2$O$_3$. © *1999 Kluwer Academic Publishers*

1. Introduction

In recent years, the researchers are trying to develop materials of nanostructured metal oxides, nitrides and carbides because of their importance in electronic and engineering applications. Zirconia (ZrO$_2$) is one among them. Zirconia is a well known material and it exhibits three polymorphic forms: cubic (c), tetragonal (t) and monoclinic (m) [1]. Products made with c or t-ZrO$_2$ have high demand in recent days. The c or t-ZrO$_2$ phase can be stabilized by partially replacing Zr by foreign atoms or by introducing the foreign atoms between intermolecular ZrO$_2$ boundaries. The compounds of Y, Ca, Mg, Ce, Bi and Al are commonly used for such stabilization [2–5]. Recently, by sol-gel process [6], Stefanovich *et al.* [7] stabilized t-ZrO$_2$ at RT with 3 mol % of Y$_2$O$_3$ and the resultant powders obtained are in nanostructured (NS) form. In NS materials, the microstructure can be easily altered because of large surface to volume ratio of the grains (crystallites). About 40% of the total atoms are located at the grain boundary surfaces of the NS specimens containing less than 10 nm size crystallites [8]. Though c or t-ZrO$_2$ phases are stabilized at room temperature, limited processing reports are available for stabilizing these phases at higher temperatures. Cubic or tetragonal phase of ZrO$_2$ is essential for making high strength zirconia based products. The processing temperature used for making such ZrO$_2$ based products is around 1300 °C. A recent report says that addition of Al$_2$O$_3$ (20 wt %)

with YSTZ, prevent the breakage of t-ZrO$_2$ symmetry above 1300 °C [9]. Hence, the authors were motivated to synthesize and investigate the physical properties of ZrO$_2$-Al$_2$O$_3$ nanocomposite system. The main motivation of the present work was to develop high dense (>98%) crack free ZrO$_2$ based products. Preparation procedure of the ZrO$_2$-Al$_2$O$_3$ nanocomposite system with various Al$_2$O$_3$ concentrations is discussed in the following section.

2. Experimental
2.1. Preparation of ZrO$_2$-Al$_2$O$_3$ nanocomposite

The nanocomposite system ZrO$_2$-Al$_2$O$_3$ with various concentrations of Al$_2$O$_3$ (5, 10 and 15%) has been prepared using sol-gel technique. Inorganic salts of Zr, Y and Al were used as precursors. First, spectroscopic grade 97 mol % zirconium (IV) tetrachloride and 3 mol % yttrium nitrate salts were dissolved in ethylene glycol solution. This solution was chosen as the solvent because of its higher boiling point (197 °C) and its easy solubility with H$_2$O [10]. The solution was stirred until the salts were completely dissolved. The solution became transparent in nature. Then, this solution was refluxed at 100 °C for 12 hours and aluminum chloride was added into the solution with suitable proportion to prepare YSTZ-Al$_2$O$_3$ (5 wt %) nanocomposite system. Again the solution was refluxed at 100 °C for the same duration. During the refluxing period NaOH was added

in impurity level. On refluxing, the basic salts reacted with ethylene glycol solution and formed their respective alkoxides. The colour of the solution changed into whitish brown. The gases evolved during this reaction were ejected out.

Then H_2O was added slowly (preferably drop by drop) into the hot solution. Hydrolysis process occurs; during this process the alkoxides decomposed into hydroxides and precipitated at the bottom of the container. The precipitate was washed with hot water for removing the adsorbed organic molecules from the surface of the precipitate. On heating, the hydroxides decomposed and the resultant product $Zr(Y, Al)O_2$ was formed. The same procedure was adopted to prepare YSTZ samples with 10 and 15 wt % Al_2O_3. Pure YSTZ was also prepared to compare the results with YSTZ-Al_2O_3 nanocomposite.

2.2. Characterization

The synthesized powders were subjected to various investigations using the experimental techniques XRD (SEIFERT), DTA (PERKIN-ELMER), TGA (PERKIN-ELMER), SEM (JEOL), Vickers microhardness tester (REICHERT), density measurements, FT-Raman (BRUKER), FT-IR (NICOLET) and Impedance analyser (SOLARTRON). XRD data were collected between $\theta = 10°$ and $35°$ using the monochromated CuK_α radiation with $0.005°$ step. The crystalline phases and cell dimensions were found from the diffraction profiles. The crystallite size was estimated from the FWHM values of the theoretically fitted diffraction profiles using the Scherrer formula [11]. Raman spectra were taken to compare the structural results found by the XRD method. FT-IR studies have been carried out to find the molecular bondings. DTA measurements were carried out in the temperature range between 500 and 1350 °C in oxygen atmosphere with a heating rate of 10 °C/min; α-alumina powder was used as reference material. Thermo Gravimetric Analyzer (TGA) was used to find the weight loss on crystallization.

Disc specimens of dimensions 1 cm in diameter and 0.2 cm in thickness have been prepared by applying a pressure of 0.5 GPa using a hydraulic press. The specimens were heat treated at various temperatures in air atmosphere for sintering. The density as a function of sintering temperature was measured using the Archimede's principle. The 1300 °C sintered specimens were polished using an automated MOTOPOL 2000 polisher and used for microhardness measurements. The indentation diagonals were measured with a help of an optical Leica microscope attached to the microhardness tester. The Vicker's hardness values were obtained using the relation $H_v = 1854.4 P/d^2$, where P is the indentation load in gram-force and d is the indentation diagonal in micrometres [12]. For impedance spectroscopy studies, both the surfaces of the sintered specimens were coated with platinum paste. The complex-impedance spectrum (Z'-Z'' plot) was recorded from 1 MHz to 100 Hz with an input signal amplitude of 0.05 V from the lock-in amplifier attached to the impedance analyzer.

3. Results

XRD studies have been carried out for the pure and Al_2O_3 doped zirconia specimens sintered at various temperatures between RT and 1300 °C. Fig. 1 shows typical XRD spectra obtained on the specimens heat treated at 100, 750, 800, 900, 1000 and 1100 °C for 3 hours. The X-ray reflection peaks are not observed for the specimens heated at 100 °C. The peaks are seen for the specimens heat treated above 750 °C with broad profiles. Well resolved reflections are obtained for the specimens heated at and above 1000 °C. X-ray line broadening studies have been carried out to find the peak position and profile width. The background data were subtracted from the intensity before fitting the profiles. The fitted results show that the values of the FWHM of the profiles decrease with sintering temperature. Line splitting corresponding to tetragonal symmetry develops for the specimens heated at 1000 °C. It was found that the total width of the splitting profiles is smaller than the corresponding width calculated for un-splitting lines for the specimens heat treated below 1000 °C. For example, the calculated FWHM values $FWHM_{(202)+(220)}$ and $FWHM_{(113)+(131)}$ for the 1000 °C heated specimens are ≈ 0.03 and ≈ 0.023 Å respectively, whereas the corresponding values calculated for the specimens heated below 1000 °C are 0.08 and 0.06 Å respectively. Also, it was observed that the addition of Al_2O_3 decreases the inter-planar spacing of t-ZrO_2. The typical fitted XRD profiles (202) and (220) of the pure and alumina doped (5, 10 and 15 wt %) YSTZ specimens heated at 1000 °C are given in Fig. 2. The difference in d-spacings $d_{(202)-(220)}$ and $d_{(113)-(131)}$ calculated for the pure YSTZ was ≈ 0.02 Å and the corresponding values for the 15 wt % Al_2O_3 doped YSTZ specimen decreases to 0.01 ± 0.001 Å. In order to calculate the cell parameters, the data obtained for the 1000 °C specimens were fitted with "least square method" using "CELN" program. The d-values and the cell dimensions coincide well with the literature values of t-ZrO_2 [13] (Table I).

Fig. 3 is the XRD spectra of the specimens heated at 1300 °C for 3 hours. The figure shows that, except for YSTZ-15% Al_2O_3, all specimens change their crystal symmetry from tetragonal to m-ZrO_2 [14]. The reflections corresponding to α-Al_2O_3 are also seen. In YSTZ-15% Al_2O_3 system, the tetragonal symmetry of

TABLE I Calculated cell dimensions of ZrO_2 in YSTZ-Al_2O_3 nanocomposite system heated at 1000 °C for 3 hours and at 1300 °C for 3 hours

Specimen	Cell dimensions (Å)		
	a	b	c
1000 °C for 3 hours			
YSTZ (pure)	5.109	5.109	5.203
YSTZ-Al_2O_3 (5%)	5.102	5.102	5.199
YSTZ-Al_2O_3 (10%)	5.101	5.101	5.196
YSTZ-Al_2O_3 (15%)	5.116	5.116	5.192
1300 °C for 3 hours			
YSTZ (pure)	5.146	5.202	5.313
YSTZ-Al_2O_3 (5%)	5.144	5.201	5.312
YSTZ-Al_2O_3 (10%)	5.140	5.200	5.311
YSTZ-Al_2O_3 (15%)	5.104	5.104	5.199
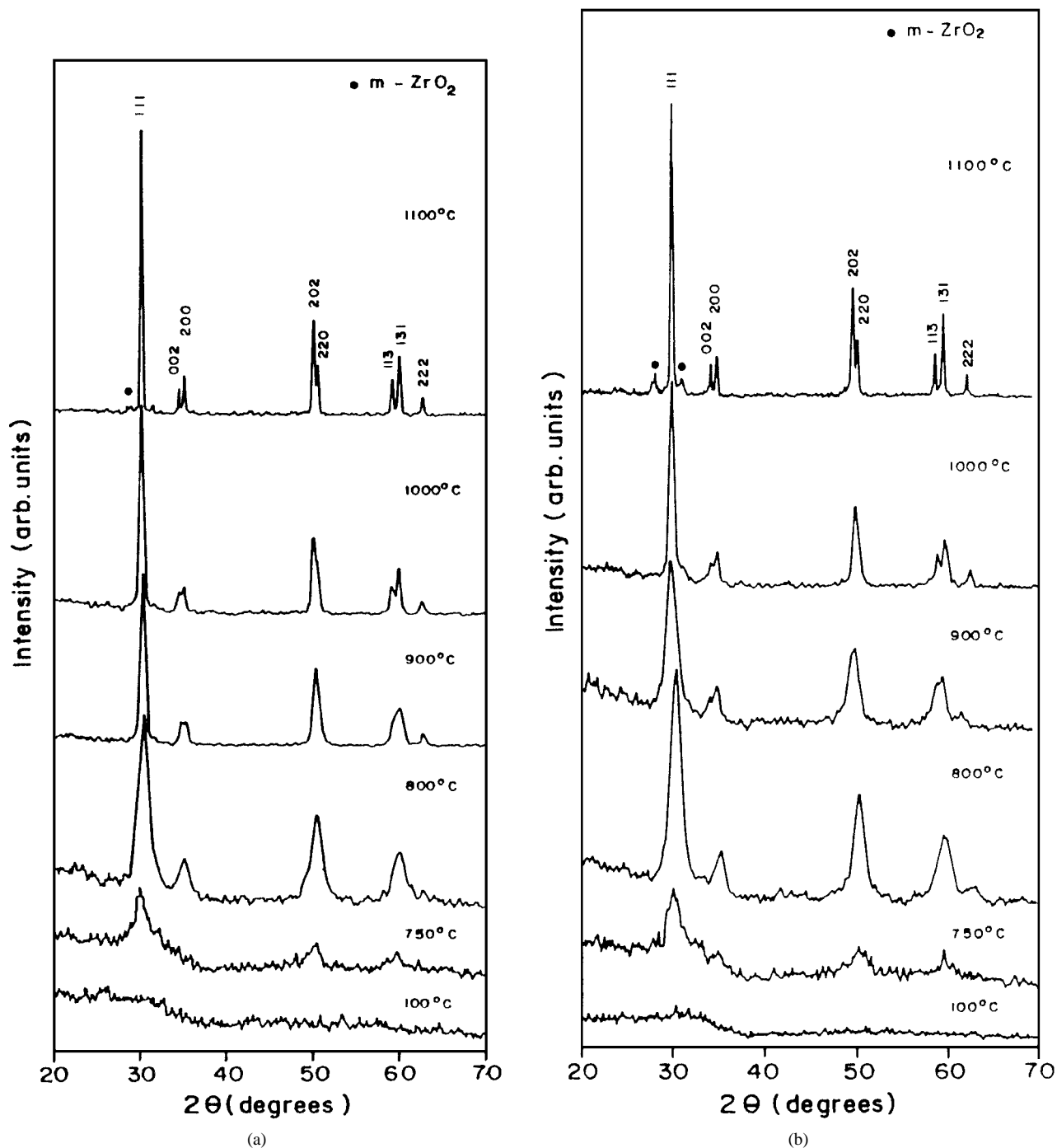
Figure 1 XRD patterns of (a) pure YSTZ, (b–d) YSTZ-Al$_2$O$_3$ (5, 10 and 15 wt %) specimens heated at 100, 750, 800, 900, 1000 and 1100 °C for 3 hours.

ZrO$_2$ remains stable up to 1300 °C. There is no evidence for the presence of m-ZrO$_2$ phase or α-Al$_2$O$_3$ in YSTZ-15%Al$_2$O$_3$ system. The calculated cell parameters for the 1300 °C heat treated specimens are given in Table I. These data indicate that the tetragonal phase is fully stabilized by addition of 15 wt % Al$_2$O$_3$ possibly due to almost complete solid solution of Al$_2$O$_3$ in ZrO$_2$ on heat treatment at 1300 °C for three hours.

The crystallite size calculated at various temperatures using the Scherrer formula is given in Table II. The data show that the size of the crystallites is in the range between 9 and 11 nm for specimens heated up to 900 °C. The crystallites start to grow with higher temperature of heat treatment. The size exceeds 50 nm when the specimens are sintered at 1300 °C.

TABLE II Crystallite size of ZrO$_2$ in YSTZ-ZrO$_2$ nanocomposite system heated at various temperatures

Specimen	Average crystallite size (nm) of ZrO$_2$ in YSTZ-Al$_2$O$_3$ heated at				
	800 °C	900 °C	1000 °C	1100 °C	1300 °C
YSTZ (pure)	10	11	27	47	58
YSTZ-Al$_2$O$_3$ (5%)	9	11	28	44	55
YSTZ-Al$_2$O$_3$ (10%)	10	11	32	50	57
YSTZ-Al$_2$O$_3$ (15%)	9	10	33	50	56

The DTA result (Fig. 4) shows two exothermic reaction peaks between 100 and 1300 °C. The onset and peak temperatures of these two exothermic peaks are given in Table III. It was observed that the onset
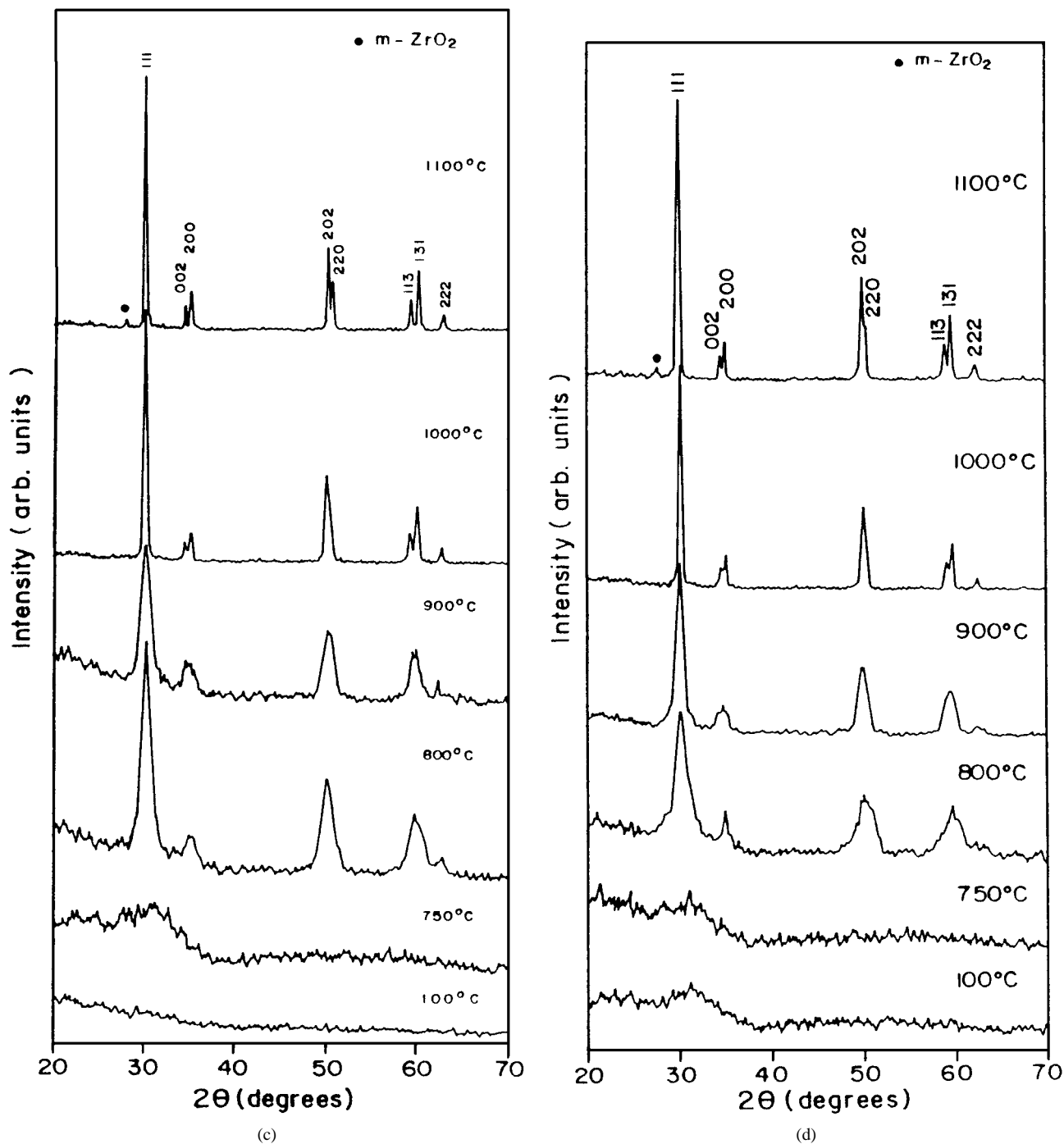
Figure 1 (Continued.)

TABLE III Onset and peak positions of the two exothermic reactions obtained from the DTA spectra of YSTZ-Al_2O_3 nanocomposite system

Specimen	First exothermic reaction temp. (°C)		Second exothermic reaction temp. (°C)	
	Onset	Peak	Onset	Peak
YSTZ (pure)	762	792	960	981
YSTZ-Al_2O_3 (5%)	766	820	961	975
YSTZ-Al_2O_3 (10%)	781	818	976	995
YSTZ-Al_2O_3 (15%)	801	824	932	1007

temperature of the first and second exothermic reactions starts at 760 and 960 °C respectively for pure YSTZ and these reaction temperatures vary with Al_2O_3 contents (Table III). These exothermic peaks correspond to the crystallization temperature of grain and grain bound-

ary regions, respectively. The possible reasons are discussed in detail in the discussion section. But, for the second reaction, the onset temperature does not change consistently with the Al_2O_3 content. It was observed from the Fig. 4 that the second exothermic peak is not well pronounced for YSTZ-15%Al_2O_3 system and that the reaction occurs over a wide temperature range. TGA result (Fig. 5) shows that a total weight loss of $\approx$4% occurred between 50 and 850 °C. The first derivative curve of the TGA traces (Fig. 6) shows three weight loss peaks: first at 100 °C, second at 320 °C and third at 420 °C. It gives an information that the specimens contain impurities like water and organic molecules which are evaporated during the heat treatment.

Fig. 7 is a plot of the bulk density value of the specimens as a function of sintering temperature. The density
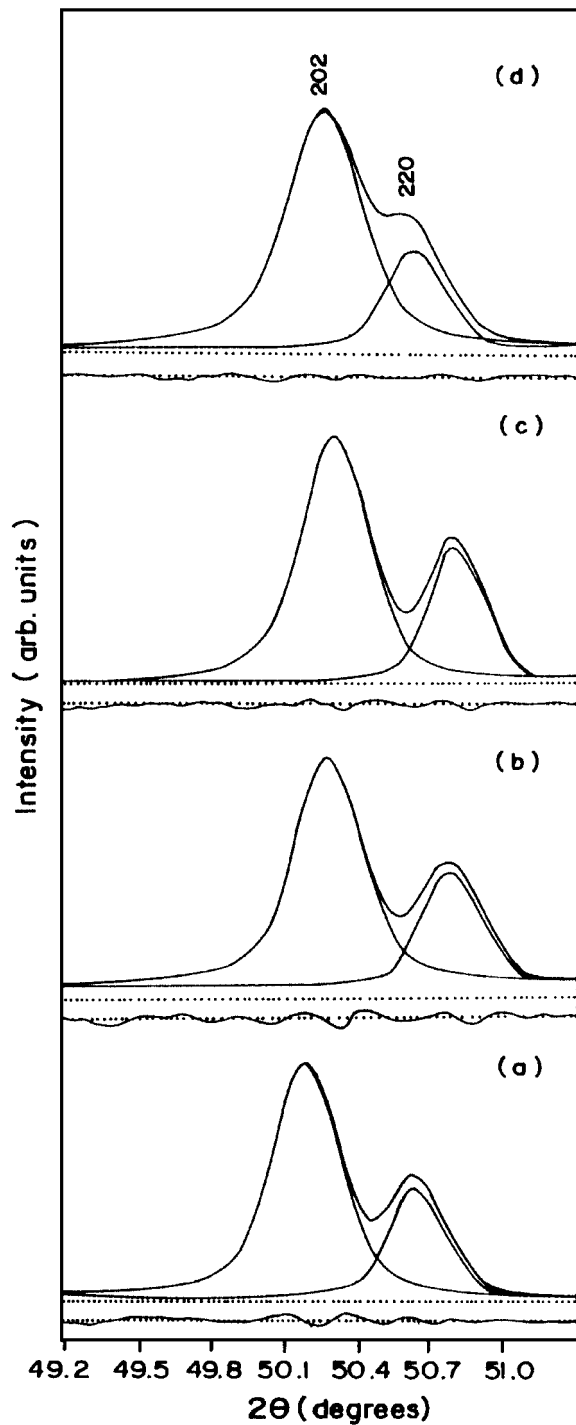
Figure 2 202 and 220 fitting reflections of (a) pure YSTZ, (b–d) YSTZ-Al_2O_3 (5, 10 and 15 wt %) specimens heated at 1000 °C for 3 hours.

value remains almost constant up to 900 °C and then increases with the increase in sintering temperature. Further, the bulk density of the sample increases with addition of Al_2O_3. Almost 100% theoretical density value (5.34 g/cm^3) was obtained for 15 wt % Al_2O_3 added specimen on sintering at 1300 °C. The specimen retains its tetragonal symmetry at 1300 °C with maximum density and high hardness value. The Vicker's hardness value obtained for this specimen sintered at 1300 °C was 1420 HV.

The objective of the present work was to stabilize the tetragonal symmetry of ZrO_2 up to its processing temperature 1300 °C for making high dense products. Hence, further studies have been carried out only with
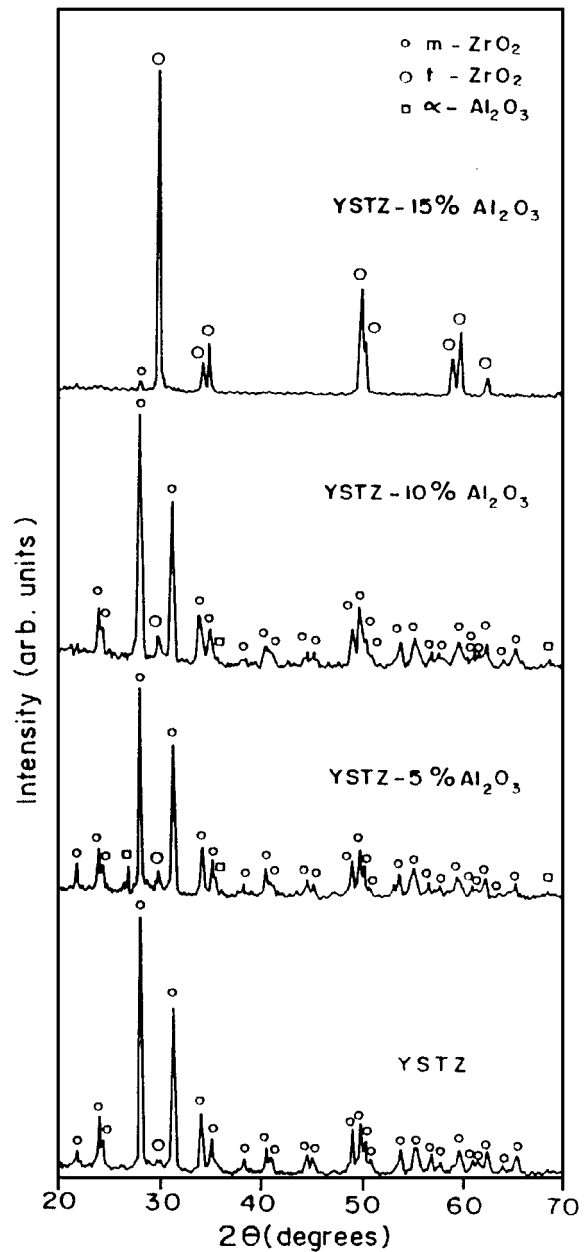
Figure 3 XRD patterns of (a) pure YSTZ, (b–d) YSTZ-Al_2O_3 (5, 10 and 15 wt %) specimens heated at 1300 °C for 3 hours.
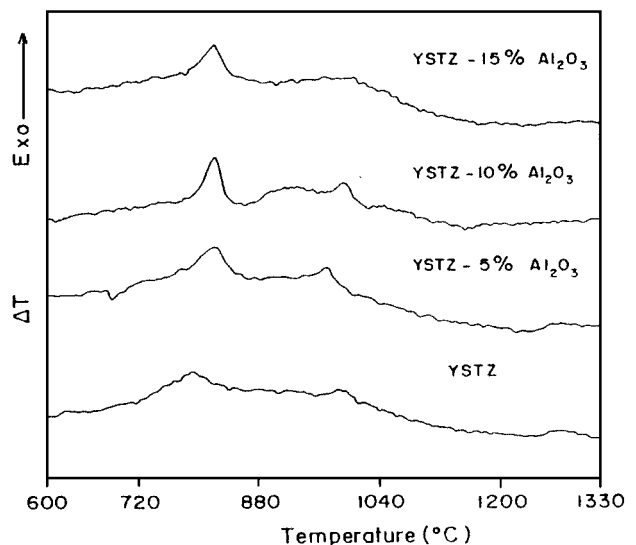
Figure 4 DTA traces of YSTZ-Al_2O_3 nanocomposite system.

2883
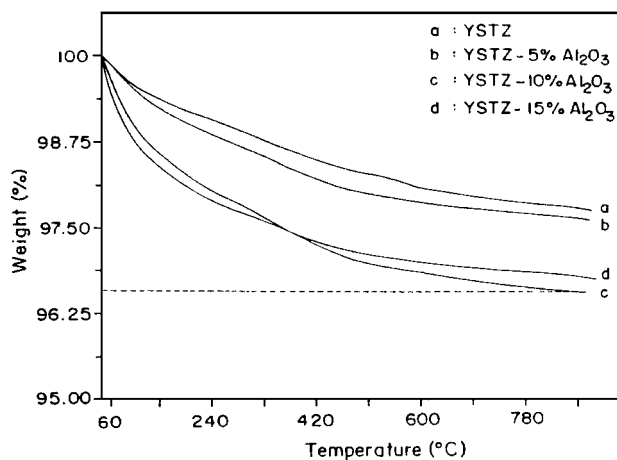
Figure 5 TGA traces of YSTZ-Al$_2$O$_3$ nanocomposite system.
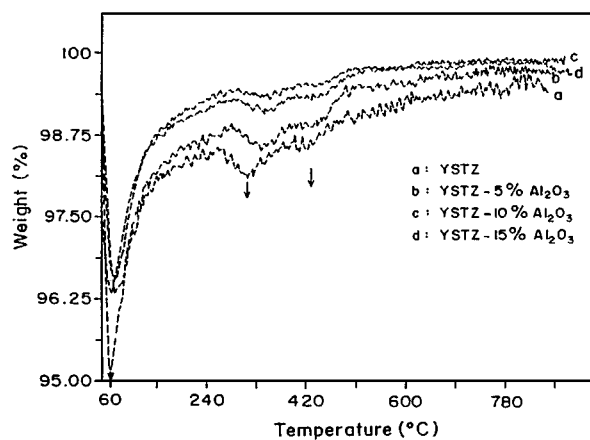
Figure 6 First derivative curves of the TGA traces in Fig. 5.
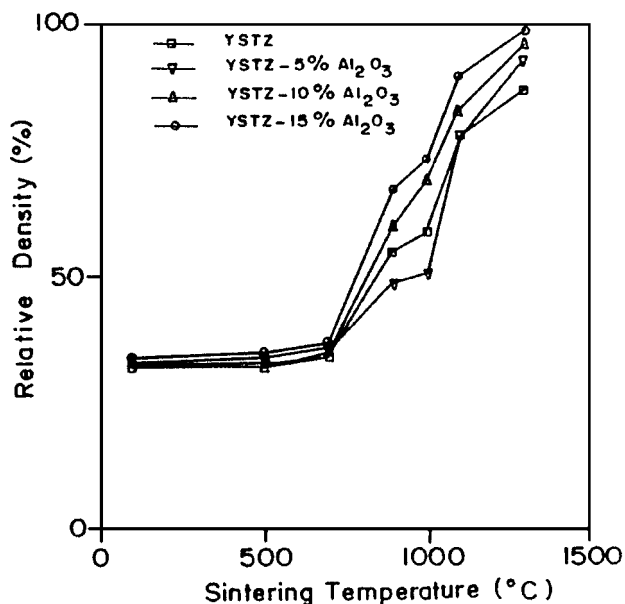
Figure 7 Effect of sintering on bulk density of YSTZ-Al$_2$O$_3$ nanocomposite system.

the specimen YSTZ-15%Al$_2$O$_3$. The results obtained from the morphological studies by SEM and spectroscopy techniques FT-Raman, FT-IR and impedance spectroscopy are discussed in the following sections.
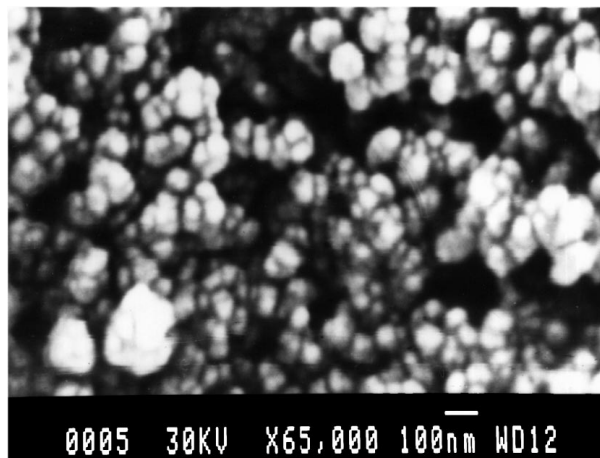
Figure 8 SEM micrograph of YSTZ-Al$_2$O$_3$ (15 wt %) specimen heated at 800 °C.

SEM micrograph of the specimen YSTZ-15%Al$_2$O$_3$ heated at 800 °C for 3 hours is shown in Fig. 8. The micrograph shows that the individual particles are spherical in shape with an average particle size of 25–50 nm. But, the crystallite size of the same specimen obtained from the line broadening studies of the XRD data was ≈10 nm. It shows that each particle is an integral assembly of ≈10 nm sized crystallites.

The FT-Raman spectra of YSTZ-15%Al$_2$O$_3$ heated at 500, 900, 1000 and 1100 °C are shown in Fig. 9. The Raman spectrum of a crystalline specimen heat treated at 500 °C shows a diffused band over a wide range of wave number from 200 to 800 cm^{-1}. No characteristic Raman bands corresponding to c or t or m-ZrO$_2$ are formed for the specimen treated at 500 °C. The specimens heat treated above 500 °C show five bands characteristic of the Raman spectrum for t-ZrO$_2$ [15].

In order to investigate the nature of chemical bonding, IR studies have been carried out for the 100 °C heated pure and 15 wt% Al$_2$O$_3$ doped YSTZ. The IR spectra taken in the transmission mode are shown in Fig. 10. The identified chemical bondings are: (O-H) stretching and vibrational bondings, (C-C), (C-H) and (M-O) bondings. It was found that the intensity of the band between 400 and 800 cm^{-1} corresponding to (M-O) bonding decreases and its centre shifts ≈20 cm^{-1} to higher frequency with the addition of alumina. But, the intensity of the other bands are constant for both pure and Al$_2$O$_3$ doped specimens. The spectra obtained are comparable with those of the reported results [1, 16] except for bands corresponding to (C-H) bondings.

Complex-impedance spectrum (Z'-Z'') of the 1300 °C sintered YSTZ-15%Al$_2$O$_3$ specimen in the frequency region between 10 MHz and 10 Hz is shown in Fig. 11a. The Z'-Z'' spectrum fits well with a single depressed semi-circle. An equivalent circuit has been generated from the R and C values obtained from the fitted semi-circle Fig. 11b. The impedance results show that the current conduction due to the boundary regions is totally absent. This means that the free volume surfaces have been removed by sintering at 1300 °C. This is in agreement with the fact that almost 100% bulk density value was obtained for this sample.
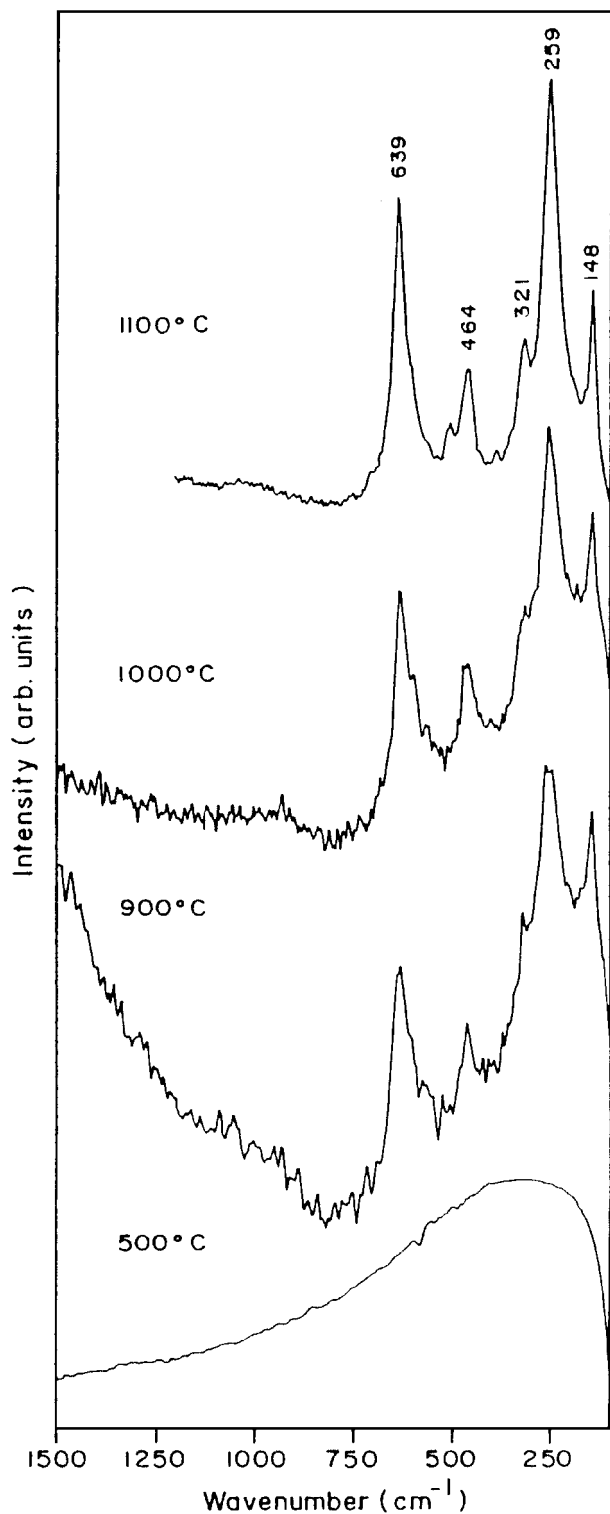
Figure 9 FT-Raman spectra of YSTZ-Al_2O_3 (15 wt %) specimen heated at 500, 800, 900, 1000 and 1100 °C.

Figure 10 FT-IR spectra of (a) pure YSTZ and (b) YSTZ-Al_2O_3 (15 wt %) heated at 100 °C.
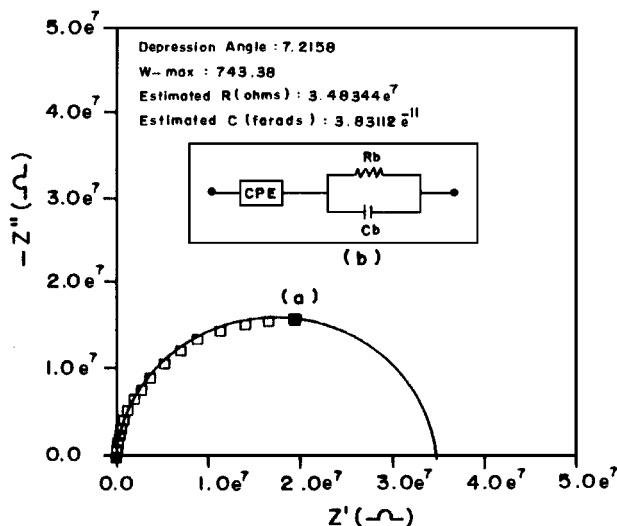
Figure 11 (a) Complex-impedance spectrum (Z'-Z'' plot) of YSTZ-Al_2O_3 (15 wt %) sintered at 1300 °C; (b) equivalent circuit generated from the fitted Z'-Z'' plot.

4. Discussion

XRD result (Fig. 1) shows that the diffraction profiles are absent for the specimens heated at 100 °C. Inter-molecular crystalline coordination starts developing on heating the specimens at 750 °C and the crystalline nature increases further with temperature. The first exothermic onset starts at 760 °C for pure YSTZ and this onset temperature increases further with Al_2O_3 contents (Table III). Well distinguished characteristic Raman bands corresponding to t-ZrO_2 develop for specimens heated above the first exothermic reaction temperature (Fig. 9). TGA result shows that the specimens contain impurity atoms and are evolved out before the first exothermic reaction temperature. FT-IR result (Fig. 10) gives an information that the existing impurities are (O-H), (C-C) and (C-H) bonded molecules. These results indicate that the removal of such impurity molecules improve the ZrO_2 intermolecular coordination and leads to t-ZrO_2 crystallization. Al_2O_3 addition decrease the intensity of the IR band corresponding to (M-O) bonding and shifts the band to higher frequency. This shows that a new molecular linkage like -O-Zr-O-Al- might have developed between Al_2O_3 and ZrO_2. Such molecular network creates new interfacial energy at the boundaries and enhance the bulk crystallization temperature. The bulk crystallization temperature increases by about 40 °C with the addition of 15 wt % Al_2O_3.

Second exothermic reaction which starts at 960 °C for the pure YSTZ also shifts to higher temperature with Al_2O_3 contents. The line broadening studies of the XRD data shows that the difference in d-spacing between the splitting profiles $d_{(202)-(220)}$ (Fig. 2) and $d_{(113)-(131)}$ decreases with Al_2O_3 contents. The variation in the splitting is clearly seen in YSTZ-15%Al_2O_3. This is an evidence that Al_2O_3 molecules interact with

ZrO$_2$ and form partial solid solution and alter the intermolecular co-ordination of ZrO$_2$. But, such variations do not seems to affect the tetragonal symmetry. Table II shows that, up to 900 °C, the size of the crystallites are in the range between 9 and 11 nm. An increase in the crystallites size was observed when the specimens were heated at 1000 °C. Also, profile splitting corresponding to the tetragonal symmetry are well resolved for the same specimens. It gives an impression that the disordered grain boundary atoms, as proposed by Gleiter [17] and Birringer *et al.* [18], probably control the growth of bulk crystallites up to 900 °C. And, above 900 °C the grain boundary atoms get themselves aligned giving a change in the interfacial energy which probably played a role for the formation of second exothermic reaction peak.

Above 1000 °C, inter-particles contact develops, hence the crystallite size increases further with temperature and exceeds 50 nm when the temperature reaches 1300 °C. At 1300 °C, the specimens undergo a structural phase transition, except YSTZ-15wt%Al$_2$O$_3$. The specimen changes its crystal symmetry from t to m-ZrO$_2$. The XRD reflections corresponding to t-ZrO$_2$ and Al$_2$O$_3$ are also present implying the formation of a composite; the intensities are around the background level. The structural modification arises due to the distortion of atomic arrangements at the particles boundary regions. This distortion may occur due to the growth of the crystallites at the particle boundary surfaces. It was observed from the SEM micrograph and line broadening studies of the XRD data that each particle is an integral assembly of nm size crystallites. When the crystallites at the particle boundary surfaces grow, amorphous nature of atomic arrangements might have existed at the bridging regions. As a result, gradient in atomic density develops between the bulk and boundary regions which might initiate distortion of the atomic arrangement. Wolf *et al.* [19] have observed that as the crystallites grow, amorphous materials exists at the boundary regions. In addition, the nature of intra-molecular (M-O) bondings in ZrO$_2$ are comparatively weaker. Due to these facts, the weakly bonded oxygen atoms are easily displaced from their original positions and forms a metastable m-ZrO$_2$ phase. But, the specimen YSTZ-15wt%Al$_2$O$_3$ remains in tetragonal symmetry at 1300 °C, even though the crystallite size exceeds 50 nm. The reflections corresponding to metastable phase m-ZrO$_2$ and Al$_2$O$_3$ are totally absent. This shows that, as the concentration of Al$_2$O$_3$ increases, the interactions of Al$_2$O$_3$ molecules with ZrO$_2$ are not weakened and Al$_2$O$_3$ stabilizes inter-molecular ZrO$_2$ bondings which prevent the nucleation of metastable phases. A hardness value of $\approx$1400 HV and maximum bulk density value (5.34 g/cm^3) were obtained for the YSTZ-15 wt % Al$_2$O$_3$ specimen.

5. Conclusion
YSTZ-Al$_2$O$_3$ nanocomposite system with various Al$_2$O$_3$ concentration has been successfully synthesized using sol-gel route. The crystallites grow on heating the specimens above 750 °C. The molecular co-ordination develops between Al$_2$O$_3$ and YSTZ, increase the crystallization temperature and enhance the structural stability of t-ZrO$_2$. The bulk grain (crystallite) and grain boundary regions are crystallized independently in two different temperature regions. High dense (about 100%) zirconia based product was obtained with the addition of 15 wt % Al$_2$O$_3$ and 1300 °C of sintering.

References
1. K. ISHIDA, K. HIROTA, O. YAMAGUCHI, H. KUME, S. INAMURA and H. MIYAMOTO, *J. Amer. Ceram. Soc.* **77** (1994) 1391.
2. K. S. MAZDIYASNI, C. T. LYNCH and H. S. SMITH, *ibid.* **49** (1966) 286.
3. L. H. SCHOENLEIN, L. W. HOBBS and A. H. HEUER, *Acta. Crystallogr.* **13** (1980) 375.
4. N. CLAUSSEN, R. WAGNER, L. J. GAUCKLER and G. PETZOR, *J. Amer. Ceram. Soc.* **61** (1978) 369.
5. R. RAMAMOORTHY, R. N. VISWANATH and S. RAMASAMY, *Bull. Electrochem.* **12** (1996) 133.
6. L. L. HENCH and J. K. WEST, *Chem. Rev.* **90** (1990) 33.
7. E. V. STEFANOVICH, A. L. SHLUGER and C. R. A. CATLOW, *Phys. Rev.* **B49** (1994) 11560.
8. N. ICHINOSE, Y. OZAKI and S. KASHU, "Superfine Particle Technology" (Springer Verlag, London, 1992).
9. G. B. PRABHU and D. L. BOURELL, *Nanostructured Materials* **6** (1995) 361.
10. CRC Hand book of Chemistry and Physics, edited by Robert C. Weast and Melvin J. Astle (CRC Press, Florida, 1981) p. C-295.
11. B. D. CULLITY, "Elements of X-ray Diffraction," 2nd ed. (Addison-Wesley, London, 1978).
12. E. L. WETZLAR, "A Guide for Working with the DURIMET Small Hardness Tester" (Ernst Leitz GmbH Wetzlar, Germany).
13. Joint Committee for Powder Diffraction Standards, X-ray Powder data file, File No: 17-923, JCPDS, Philadelphia, 1980.
14. Joint Committee for Powder Diffraction Standards, X-ray Powder data file, File No: 13-307, JCPDS, Philadelphia, 1980.
15. R. SRINIVASAN, M. B. HARRIS, S. F. SIMPSON and R. J. DE ANGELIS, *J. Mater. Res.* **3** (1988) 787.
16. H. YOSHIMATSU, T. YABUKI and H. KAWASAKI, *J. Non Cryst. Sol.* **100** (1988) 413.
17. H. GLEITER, in Proceedings of the 2nd Riso International Symposium on Metallurgy and Materials Science, edited by N. Hansen, A. Horsewell and T. Leffers (Roskilde, 1981) p. 15.
18. R. BIRRINGER, H. GLEITER, H. P. KLEIN and P. MARQUARDT, *Phys. Lett.* **102A** (1984) 365.
19. D. WOLF, J. WANG, S. R. PHILLPOT and H. GLEITER *ibid.* **A205** (1995) 274.